

RESEARCH ARTICLE

User-Centric Joint Beamforming for Multi-Antenna UAV Networks With 3D Blockage Effects

XIANMING ZHAO¹, YUTING ZHU¹², (Student Member, IEEE),
AND HONGTAO ZHANG¹², (Senior Member, IEEE)

¹Harbin Institute of Technology, Harbin 150006, China

²Key Laboratory of Universal Wireless Communications, Ministry of Education of China, Beijing University of Posts and Telecommunications, Beijing 100876, China

Corresponding author: Hongtao Zhang (htzhang@bupt.edu.cn)


This work was supported in part by Beijing Natural Science Foundation under Grant L212028, and in part by the National Natural Science Foundation of China under Grant 61971064.

ABSTRACT In unmanned aerial vehicle (UAV) networks, introducing multiple-input/multiple-output (MIMO) technology brings promising capacity gains by exploiting spatial multiplexing. However, for UAV communications in urban scenarios, dense buildings block air-to-ground links, which leads to non-consistent service for users. In this paper, a user-centric joint beamforming design for multi-UAV networks aiming at maximizing the sum-rate performance is proposed, where the distributed antennas are deployed in UAV clusters forming virtual MIMO links to seamlessly guarantee user service under the 3D blockage effect. Specifically, the UAV clusters are constructed dynamically in a user-centric way for cooperative transmissions, which are dominated by the line-of-sight (LoS) connections considering building blockage effects. In addition, the selected user-to-UAV links must be less affected by the building blockages which are measured through the established channel model from comprehensive dimensions including sizes, locations, and heights. Within the UAV clusters, the proposed joint beamforming is performed based on the majorization-minimization (MM) algorithm for the NP-hard problem under per-antenna power constraints, and the optimal UAV parameters including UAV placement and antenna configuration with a fixed total number of antennas are investigated under different blockage effect. Simulation results demonstrate that the proposed design can improve sum-rate performance by more than $1\times$ compared with single UAV deployment under densely-located building environments.

INDEX TERMS Unmanned aerial vehicle, user-centric joint beamforming, 3D blockage effects, majorization-minimization, multi-antenna configuration.

I. INTRODUCTION

Unmanned aerial vehicle (UAV), as an emerging technology, has drawn growing attention over the past few years due to its advantage of autonomy, flexibility, and air-to-ground capability [1]. It enables diverse applications ranging from delivery and communications to surveillance, inspection, and transportation [2], [3]. Among its numerous application domains, wireless communication is essential where UAV can act as different roles such as a new aerial platform [4], [5] or a user equipment [6]. Particularly, as an

The associate editor coordinating the review of this manuscript and approving it for publication was Wei Feng .

aerial base station, UAV can be installed with multiple antennas to collaboratively serve users through flexible beamforming [7], enabling enhancement of network access and reliable services [8]. Given the air-to-ground advantage, the altitude of UAV can also be optimized to fulfill the capacity improvement potential of UAV communication [9], [10]. However, when operating in urban environments, the UAV network encounters distinctive challenges.

The intricate and densely populated urban landscape introduces obstacles that impede the wireless communication link from a single UAV. These impediments not only diminish the effectiveness of the beamforming techniques but also lead to inconsistent services for end-users. Due to

the high mobility and line-of-sight (LoS) feature of UAV networks, the channel quality fluctuates, and therefore, the wireless communication link from a single UAV [11] can not guarantee the consistency of service. The need for innovative solutions becomes paramount to address connectivity issues and optimize the system performance of UAV communication in urban scenarios.

A. RELATED WORKS

To guarantee the user's quality of service, the multiple UAV-aided network [12], [13], [14] is necessary to be discussed for breaking through the limited capability of a single UAV. In the multi-UAV scenario, the LoS feature leads to serious interference among UAV communication links, while most works avoid handling the interference through power control or orthogonal resource block allocation [12]. From the perspective of optimization, the work in [14] manages the interference by using deep reinforcement learning (DRL) to optimize the association and beamforming design jointly. DRL has also been widely employed in trajectory design, scheduling and power control of UAV-assisted networks [15], [16], but this approach needs an extra offline training phase. To deal with the interference and further exploit the additional multiplexing gains, the coordinated transmission with multiple-input multiple-output (MIMO) techniques is an imperative solution, proved in [17] and [18] without adopting an extra training process. By capitalizing on the spatial degree of freedom, UAVs are equipped with multiple antennas to collaboratively transmit information to multiple users through joint beamforming. Within a cooperative group of UAVs, the channel state information (CSI) of all users is shared to support the beamforming scheme. This collaborative effort leads to a substantial improvement in system performance over the single-input single-output (SISO) system in terms of coverage and throughput [19]. Therefore, with coordinated UAVs, joint transmissions through proper clustering and beamforming are required crucially to realize interference mitigation [20]. However, in this dense urban environment, the traditional static coordination clustering is no longer applicable because the performance will be severely affected by the poor network connectivity caused by the building blockages.

To overcome the effects of blockages, it is worth mentioning that a promising technology named reconfigurable intelligent surface (RIS) has been proposed to be able to reconstruct desirable LoS links, also in UAV-aided networks [4], [21], [22]. However, although RISs are appealing for future applications, their implementation still faces significant challenges [23]. Apart from this, a novel idea called user-centric clustering is to be mentioned. It was first introduced to mitigate the cluster-edge effects and enhance the performance of all users in cooperative networks [24], bringing substantial cooperative gain, especially in a situation where access points are densely deployed. The user-centric overlapped clustering schemes shows great advantage over the non-overlapped clustering counterpart in terms of the

throughput of the edge users [25]. Considering the fact that the user-centric clustering design can flexibly organize the required serving group to provide seamless coverage [26], [27], we employ the user-centric coordinated transmission scheme for UAV network under air-to-ground channels and the blockage effect for capacity enhancement.

With the advance of distributed antenna system [28], which lowers the correlation between antennas and increases the spatial diversity, multiple UAVs equipped with several antennas can effectively improve network capacity, with user-centric joint beamforming design to form a virtual MIMO link. Reference [29] proposed a coordinated multi-antenna UAV network to enhance throughput via multi-cell beamforming, but the severe impact of blockage on UAV coordination clustering and beamforming design have never been considered. References [30] and [31] proposed a blockage model and performed interference coordination under the blockage effect in UAV networks through stochastic geometry, but it only gave a theoretic analysis under the assumption of a single antenna. The work in [32] provides a performance analysis of vertical heterogeneous networks with multiple UAVs under blockage effects and MIMO systems. Since the system of multi-UAVs equipped with distributed antennas brings higher cost and higher energy consumption, it is yet unclear what is the most cost-effective UAV antenna deployment in dense urban areas. Thus, how to realize the sum-rate maximization of the multi-user system under the blockage effect in multi-antenna UAV networks through beamformer design and specific UAV parameters, which refer to UAV placement and antenna deployment with a fixed total number of antennas, is still a significant open problem.

B. CONTRIBUTIONS

In this article, we propose a user-centric UAV joint beamforming design based on the established three-dimensional (3D) blockage model and evaluate the sum-rate performance under different UAV parameters with per-antenna power constraints. In detail, we consider a multi-user system where each user may be served by several cooperating UAVs only relying on the channel state information (CSI) exchanged among the cooperating UAVs. The cooperating UAVs based on the user-centric framework form dynamic serving clusters, of which size is also discussed in this article. Numerical results show that the proper UAV parameters and beamformer design can achieve higher capacity gains in denser urban areas. The contributions of this article are summarized as follows:

- Considering the urban environment with random blockages, we utilize the proposed 3D blockage model which fully exploits the dimension relationships among UAVs, users, and buildings. The blockages cause poor channel conditions and eventually affect the user-centric clustering organization, which is practical in the urban scenario.

TABLE 1. Acronyms used in this paper.

Acronyms	Text
AoA	Angle of arrival
AoD	Angle of departure
CSCG	Circularly symmetric complex Gaussian
CSI	Channel state information
LoS	Line-of-sight
MIMO	Multiple-input multiple-output
MM	Majorization-minimization
MMSE	Minimum mean-square error
MSE	Mean-square error
NP	Non-deterministic Polynomial
PPP	Poisson point process
RIS	Reconfigurable intelligent surface
SINR	Signal-to-interference-plus-noise ratios
SISO	Single-input single-output
SVD	Singular value decomposition
UAV	Unmanned aerial vehicle
UAVG	Unmanned aerial vehicle group
ULA	Uniform linear array
2D	Two-dimensional
3D	Three-dimensional

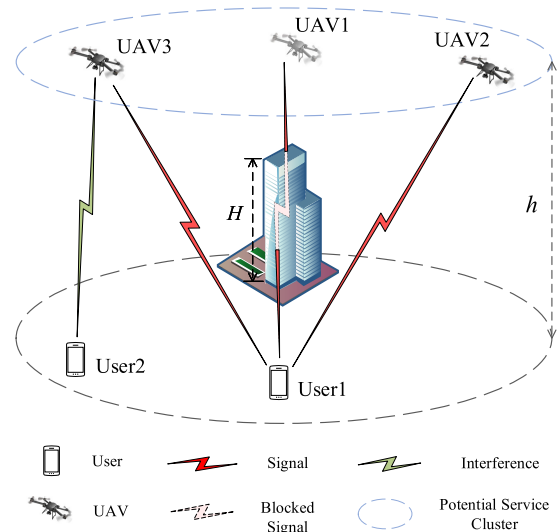


FIGURE 1. Illustration of the system model with densely located buildings in UAV networks. The closest UAV1 cannot be chosen to serve user1 due to the building blockage, and in this dense urban area, UAV2 and UAV3 will form a user-centric serving cluster to guarantee the user's service. The signal transmitted from UAV3 to user2 will be regarded as interference for user1.

TABLE 2. Notations.

Symbol	Definitions
$\mathbb{E}[\cdot]$	The expectation operation
$(\cdot)^T, (\cdot)^H$	The transpose and Hermitian operators
\triangleq	The definition operator
$\det(\cdot)$	The determinant operator
$[\mathbf{A}]_{i,j}$	The (i,j) -th element in matrix \mathbf{A}
$\text{Tr}(\mathbf{A})$	The trace of \mathbf{A}
$\mathbb{C}^{a \times b}$	The space of $a \times b$ complex matrices
$\mathcal{CN}(\mathbf{x}, \Sigma)$	The distribution of a circularly symmetric complex Gaussian (CSCG) random vector with mean vector \mathbf{x} and covariance matrix Σ
$\mathbf{I}, \mathbf{0}$	An identity matrix and an all-zero matrix with appropriate dimensions
$\nabla_{\mathbf{x}}$	The gradient with respect to \mathbf{X}
$\text{diag}(\cdot)$	The diagonalization operation
\mathcal{O}	The big-O notation

- A user-centric joint beamforming design is derived to deal with the optimization problem of sum-rate maximization under per-antenna power constraints. With the limited CSI in the cooperating cluster, the proposed design effectively mitigates the intra-cluster interference and explores the cooperation gain under the different sizes of clusters.
- In order to evaluate the potential gain of the distributed antenna system in UAV communication, different UAV parameters including number and antenna deployment are discussed under different blockage scenes. With the fixed total numbers of antennas deployed to different number of UAVs, the systems with these antenna deployments perform diversely and the distributed one outperforms the centralized one under severe blockage effect in dense scenes revealed by the simulation result.

The remainder of this article is organized as follows: Section II describes the system model, and the channel model with blockage effect, and further presents a constrained optimization problem. In Section III, a user-centric joint beamforming design is proposed based on the limited CSI in the clusters. Section IV presents the simulation results and performance discussions. The conclusions of this article are finally shown in Section V. Table 1 summarizes all acronyms used in this paper.

II. PRELIMINARIES

A. SYSTEM MODEL

As shown in Fig. 1, we consider a UAV network under densely located buildings with the 3D blockage effect. We model the random buildings with a comprehensive characterization of the random blockages, such as height, location, and orientation. The heights of buildings follow a Rayleigh distribution with the mean $\mathbb{E}[H]$ while the average length and width are denoted as $\mathbb{E}[L]$ and $\mathbb{E}[W]$ respectively. The centers of buildings are generated according to a two-dimensional (2D) Poisson point process (PPP) with

density λ in the area and $p = \lambda \mathbb{E}[L] \mathbb{E}[W]$ refers to the index of city density denoting the ratio of buildings area to the total land area. M_0 antennas are allocated to $\mathcal{K} = \{1, 2, \dots, K\}$ UAVs distributedly. UAVs, each equipped with $M = M_0/K$ antennas that form a uniform linear array (ULA), are positioned outside buildings of height h , serving $\mathcal{I} = \{1, 2, \dots, I\}$ users. Each user is equipped with a ULA consisting of N antennas in this network. The main notations used throughout this paper are summarized in Table 2.

Let $\mathbf{H}_{ik} \in \mathbb{C}^{N \times M}$ represent the baseband channel spanning from the k -th UAV to the i -th user, which indicates the condition of channel state information (CSI) as well. $\mathbf{V}_{ik} \in \mathbb{C}^{M \times d_i}$ represents the beamforming matrix that the UAV k uses for the signal transmission to the user i . Then, the signal transmitted by the k -th UAV is given by

$$\mathbf{x}_k = \sum_{i=1}^I \mathbf{V}_{ik} \mathbf{s}_i, \quad (1)$$

where $\mathbf{s}_i \in \mathbb{C}^{d_i \times 1}$ presents d_i desired data streams for user i satisfying $\mathbf{s}_i \sim \mathcal{CN}(\mathbf{0}, \mathbf{I}_{d_i})$.

With the aforementioned definitions, the overall CSI between user i and all UAVs can be denoted as $\mathbf{H}_i = [\mathbf{H}_{i1}, \mathbf{H}_{i2}, \dots, \mathbf{H}_{iK}]$. Correspondingly, the collection of beamforming matrices from all UAVs to user i is expressed as $\mathbf{V}_i = [\mathbf{V}_{i1}^T, \mathbf{V}_{i2}^T, \dots, \mathbf{V}_{iK}^T]^T$. Then, under the ideal assumption that all UAVs serve all users, the signal \mathbf{y}_i received by user i , $\forall i \in \mathcal{I}$ can be expressed as

$$\mathbf{y}_i = \mathbf{H}_i \mathbf{V}_i \mathbf{s}_i + \sum_{j \neq i}^I \mathbf{H}_i \mathbf{V}_j \mathbf{s}_j + \mathbf{n}_i, \quad (2)$$

where $\mathbf{n}_i \in \mathbb{C}^{N \times 1}$ represents the additive white Gaussian noise with distribution $\mathcal{CN}(\mathbf{0}, \sigma^2 \mathbf{I})$.

B. CHANNEL MODEL WITH BLOCKAGE EFFECT

With the densely located buildings, the line-of-sight (LoS) channels between users and UAVs will be severely affected by the building blockages and we employ the blockage model described with Bernoulli variable [33]. Then, the channel matrix \mathbf{H}_{ik} can be expressed as

$$\mathbf{H}_{ik} = w_{i,k} \sum_{l=1}^{L_{ik}} g_{i,k,l} \mathbf{b}(\theta_{i,k}) \mathbf{a}(\theta_{i,k})^H, \quad (3)$$

where $\mathbf{a}(\theta_{i,k})$ and $\mathbf{b}(\theta_{i,k})$ stand for the normalized steering vectors for angle of departure (AoD) at UAV k and angle of arrival (AoA) at the receiving user i respectively, which can be given by

$$\mathbf{a}(\theta_{i,k}) = \sqrt{\frac{1}{M}} \left[1, e^{-j \frac{2\pi d_c \cos \theta_{i,k}}{\lambda_c}}, \dots, e^{-j \frac{2\pi d_c (M-1) \cos \theta_{i,k}}{\lambda_c}} \right]^T,$$

$$\mathbf{b}(\theta_{i,k}) = \sqrt{\frac{1}{N}} \left[1, e^{-j \frac{2\pi d_c \cos \theta_{i,k}}{\lambda_c}}, \dots, e^{-j \frac{2\pi d_c (N-1) \cos \theta_{i,k}}{\lambda_c}} \right]^T.$$

λ is the wave-length, d_c is the antenna spacing, L_{ik} is the total number of paths, $g_{i,k,l}$ is the complex gain of path l and $\theta_{i,k,l}$ represents the altitude angle of UAV k to user i .

In order to describe the blockage status of the link from UAV k to user i , the coefficient $w_{i,k}$ is introduced, which represents the power loss caused by blockage closely related to the 3D relationship among the buildings, objective user, and UAV. Assuming that the signal cannot penetrate buildings in this paper, we have

$$w_{i,k} = \begin{cases} 0 & \text{if the link from UAV } k \text{ to user } i \text{ is blocked} \\ 1 & \text{otherwise.} \end{cases}$$

To be specific, the link is assumed to be blocked if there exists at least one building satisfying both conditions below:

- The link's horizontal projection falls on the area where the building is located.
- The building with height H bigger than $h_u = \frac{uh}{d}$, where the parameters u, h, d are shown in Fig. 2.

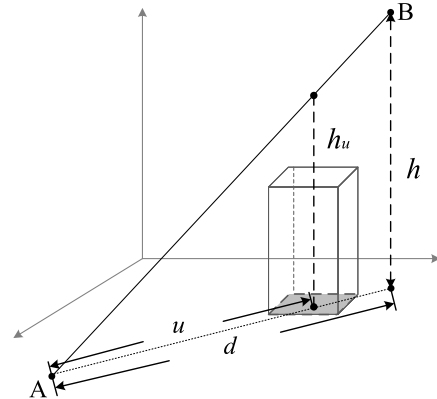


FIGURE 2. Illustration of the 3D blockage model for one link case. The horizontal distance of link AB is d . A building intersects the projection of link AB at the point which is at a horizontal distance u away from A.

C. USER-CENTRIC JOINT BEAMFORMING PROBLEM FORMULATION

The user-centric UAV coordination architecture is adopted in this article where a dynamic UAV group (UAVG) is organized for each user to transmit the same data through beamforming, aiming at providing seamless services under blockage effect. To this end, the notation $\mathcal{C}_i \subseteq \mathcal{K}$ is defined to represent the UAVG selected by user i according to the link condition. Due to the fact that the conditions of links are affected by the blockages, the UAVG \mathcal{C}_i tends to exclude the blocked UAVs.

It is assumed that for each user, considering the blockage effect as well as the user-centric architecture, only the channel information towards their serving UAVs (i.e. $\mathbf{H}_{ik}, \forall k \in \mathcal{C}_i$ and $\mathbf{H}_{ik} = 0, \forall k \notin \mathcal{C}_i$) are known in the serving cluster. By introducing an indicator function [13]

$$\mathbb{1}_{\mathcal{C}_i}(k) = \begin{cases} 1 & \text{if and only if } k \in \mathcal{C}_i \\ 0 & \text{otherwise,} \end{cases} \quad (4)$$

we can rewrite \mathbf{H}_{ik} and \mathbf{H}_i as

$$\bar{\mathbf{H}}_{ik} \triangleq \mathbb{1}_{\mathcal{C}_i}(k) \mathbf{H}_{ik}$$

$$\bar{\mathbf{H}}_i \triangleq [\mathbb{1}_{\mathcal{C}_i}(1) \mathbf{H}_{i1}, \mathbb{1}_{\mathcal{C}_i}(2) \mathbf{H}_{i2}, \dots, \mathbb{1}_{\mathcal{C}_i}(K) \mathbf{H}_{iK}], \quad (5)$$

for the beamforming design in the serving cluster \mathcal{C}_i .

With the undesired LoS feature causing severe inter-cell and intra-cell interference, the transmit beamforming within this UAVG should be designed carefully to decrease this interference and further enhance the overall system performance. In this work, the design of cluster construction and transmit beamformer is optimized in the UAVG to realize sum-rate performance maximization for all users. Note that the rate of user i can be denoted as

$$R_i = \log \det \left(\mathbf{I} + \bar{\mathbf{H}}_i \mathbf{V}_i \mathbf{V}_i^H \bar{\mathbf{H}}_i^H \left(\sum_{j \neq i}^I \bar{\mathbf{H}}_i \mathbf{V}_j \mathbf{V}_j^H \bar{\mathbf{H}}_i^H + \sigma^2 \mathbf{I} \right)^{-1} \right). \quad (6)$$

Then, the optimization problem can be established as follows:

$$\begin{aligned} & \max_{\mathbf{V}} \sum_{i \in \mathcal{I}} R_i \\ & \text{s.t. C1: } \left[\sum_{i \in \mathcal{I}} \mathbf{V}_{ik} \mathbf{V}_{ik}^H \right]_{m,m} \leq P_{km}, m = 1, \dots, M, \quad \forall k \in \mathcal{K}, \\ & \text{C2: } \mathbf{V}_{ik} = \mathbf{0}, \quad \forall k \notin \mathcal{C}_i, \quad \forall i \in \mathcal{I}, \end{aligned} \quad (7)$$

where C1 denotes the per-antenna power constraint for each UAV, C2 implies the UAV out of serving group \mathcal{C}_i will not send signal to user i and \mathbf{V} is defined as $\mathbf{V} = [\mathbf{V}_1, \mathbf{V}_2, \dots, \mathbf{V}_I]$ for expression simplicity.

III. USER-CENTRIC JOINT BEAMFORMING DESIGN

This section proposes a user-centric joint beamforming design for the optimization problem (7). Note that the objective of this problem involves multiple fractional signal-to-interference-plus-noise ratios (SINRs). However, solving multiple-ratio fractional programming is NP-hard [34]. In this paper, we present an effective algorithm to deal with it, adopting the majorization-minimization (MM) algorithmic framework to find a surrogate convex function lower bound the objective function down to a constant. Inspired by [18] and [35], we explore the relationship between user rate and mean-square error (MSE) matrix in the following.

Considering that the estimated signal vector at user i through a linear receiving filter $\mathbf{U}_i \in \mathbb{C}^{N \times d_i}$ can be expressed by $\tilde{\mathbf{s}}_i = \mathbf{U}_i^H \mathbf{y}_i$, the MSE matrix \mathbf{E}_i at user i can be formulated as

$$\begin{aligned} \mathbf{MSE}_i &= \mathbb{E}_{\mathbf{s}, \mathbf{n}} \left[(\tilde{\mathbf{s}}_i - \mathbf{s}_i)(\tilde{\mathbf{s}}_i - \mathbf{s}_i)^H \right] \\ &= \left(\mathbf{I} - \mathbf{U}_i^H \bar{\mathbf{H}}_i \bar{\mathbf{H}}_i \mathbf{V}_i \right) \left(\mathbf{I} - \mathbf{U}_i^H \bar{\mathbf{H}}_i \bar{\mathbf{H}}_i \mathbf{V}_i \right)^H \\ &\quad + \sum_{j \neq i}^I \mathbf{U}_i^H \bar{\mathbf{H}}_i \mathbf{V}_j \mathbf{V}_j^H \bar{\mathbf{H}}_i^H \mathbf{U}_i + \sigma^2 \mathbf{U}_i^H \mathbf{U}_i, \end{aligned} \quad (8)$$

under the assumption that the received signal \mathbf{s}_i and the noise \mathbf{n}_i are independent. Upon fixing each of the transmit beamformers, minimizing the sum-MSE leads to the well-known minimum MSE (MMSE) receive filter, shown as [18]

$$\mathbf{U}_i^{\text{mmse}} = \left(\sum_{j=1}^I \bar{\mathbf{H}}_i \mathbf{V}_j \mathbf{V}_j^H \bar{\mathbf{H}}_i^H + \sigma^2 \mathbf{I} \right)^{-1} \bar{\mathbf{H}}_i \mathbf{V}_i. \quad (9)$$

Thus, by substituting $\mathbf{U}_i^{\text{mmse}}$ into the MSE matrix, it can be expressed as \mathbf{E}_i :

$$\begin{aligned} \mathbf{E}_i &= \mathbf{MSE} \left(\mathbf{U}_i^{\text{mmse}} \right) \\ &= \mathbf{I} - \mathbf{V}_i^H \bar{\mathbf{H}}_i^H \left(\sum_{j \in \mathcal{I}} \bar{\mathbf{H}}_i \mathbf{V}_j \mathbf{V}_j^H \bar{\mathbf{H}}_i^H + \sigma^2 \mathbf{I} \right)^{-1} \bar{\mathbf{H}}_i \mathbf{V}_i. \end{aligned} \quad (10)$$

Let $\mathbf{N}_i = \sum_{j \neq i}^I \bar{\mathbf{H}}_i \mathbf{V}_j \mathbf{V}_j^H \bar{\mathbf{H}}_i^H + \sigma^2 \mathbf{I}$ represent the covariance matrix of the sum of the interference and noise signals received at user i . By utilizing the relation between R_i and

the MSE matrix \mathbf{E}_i , the objective function can be further expressed as [18]

$$\begin{aligned} R_i &= \log \det \left(\mathbf{I} + \bar{\mathbf{H}}_i \mathbf{V}_i \mathbf{V}_i^H \bar{\mathbf{H}}_i^H \mathbf{N}_i^{-1} \right) \\ &= \log \det \left(\mathbf{E}_i^{-1} \right). \end{aligned} \quad (11)$$

Then, we exploit the essence of the MM algorithm [36] to solve the problem here, which is widely used for non-convex optimization problems in wireless communications. The main idea is to construct a series of more tractable sub-problems to reach an approximate solution to the intractable original problem. In the following, we aim to find the suitable surrogate function first. By using the first-order condition of the above formula, we can obtain the inequality below, denoted as

$$\begin{aligned} \log \det \left(\mathbf{E}_i^{-1} \right) &\geq \log \det \left(\left(\mathbf{E}_i^{(r)} \right)^{-1} \right) \\ &\quad - \text{Tr} \left(\left(\mathbf{E}_i^{(r)} \right)^{-1} \left(\mathbf{E}_i - \mathbf{E}_i^{(r)} \right) \right) \\ &\geq \log \det \left(\left(\mathbf{E}_i^{(r)} \right)^{-1} \right) \\ &\quad - \text{Tr} \left(\left(\mathbf{E}_i^{(r)} \right)^{-1} \left(\mathbf{MSE}_i - \mathbf{E}_i^{(r)} \right) \right), \end{aligned} \quad (12)$$

where the $\mathbf{E}_i^{(r)}$ represents \mathbf{E}_i in (10) with fixed beamformer $\mathbf{V}_i^{(r)}$ and the superscript (r) means that the corresponding value is the result in the r -th iteration. Then, the optimization problem can be reformulated as

$$\begin{aligned} & \max_{\mathbf{V}} \sum_{i \in \mathcal{I}} \left(\log \det \left(\left(\mathbf{E}_i^{(r)} \right)^{-1} \right) \right. \\ & \quad \left. - \text{Tr} \left(\left(\mathbf{E}_i^{(r)} \right)^{-1} \left(\mathbf{MSE}_i - \mathbf{E}_i^{(r)} \right) \right) \right) \\ & \text{s.t. C1: } \left[\sum_{i \in \mathcal{I}} \mathbf{V}_{ik} \mathbf{V}_{ik}^H \right]_{m,m} \leq P_{km}, m = 1, \dots, M, \quad \forall k \in \mathcal{K}, \\ & \text{C2: } \mathbf{V}_{ik} = \mathbf{0}, \quad \forall k \notin \mathcal{C}_i, \quad \forall i \in \mathcal{I}, \end{aligned} \quad (13)$$

Let $f(\mathbf{V})$ denote $\log \det \left(\mathbf{E}_i^{-1} \right)$ and $g(\mathbf{V} | \mathbf{V}^{(r)})$ denote the formula

$$\log \det \left(\left(\mathbf{E}_i^{(r)} \right)^{-1} \right) - \text{Tr} \left(\left(\mathbf{E}_i^{(r)} \right)^{-1} \left(\mathbf{MSE}_i - \mathbf{E}_i^{(r)} \right) \right) \quad (14)$$

which is derived at the end of the inequality (12). It satisfies the following three conditions

$$g \left(\mathbf{V} | \mathbf{V}^{(r)} \right) \leq f \left(\mathbf{V} \right), \quad (15)$$

$$g \left(\mathbf{V}^{(r)} | \mathbf{V}^{(r)} \right) = f \left(\mathbf{V}^{(r)} \right), \quad (16)$$

$$\nabla_{\mathbf{V}} g \left(\mathbf{V} | \mathbf{V}^{(r)} \right) \Big|_{\mathbf{V}=\mathbf{V}^{(r)}} = \nabla_{\mathbf{V}} f \left(\mathbf{V} \right) \Big|_{\mathbf{V}=\mathbf{V}^{(r)}}. \quad (17)$$

The first inequality (15) means the objective function $g(\mathbf{V} | \mathbf{V}^{(r)})$ constructed should represent the lower bound of the origin function $f(\mathbf{V})$. The second and third equations,

(16) and (17), represent that the newly constructed function and its first-order gradient are the same as the original function and its first-order gradient at point $\mathbf{V}^{(r)}$. So that according to [36], the convex function $g(\mathbf{V}|\mathbf{V}^{(r)})$ can be regarded as the surrogate function of the origin objective function (10) and can be optimized in the following to obtain a stationary point through iteration, whose convergence has been proved in [36].

By substituting (8) into the surrogate function and after a series of formula transformations, it can be written as

$$\begin{aligned}
 &g(\mathbf{V}|\mathbf{V}^{(r)}) \\
 &= \sum_i \left(c_i^{(r)} + \text{Tr} \left((\mathbf{E}_i^{(r)})^{-1} (\mathbf{U}_i^{(r)})^H \bar{\mathbf{H}}_i \mathbf{V}_i \right) \right. \\
 &\quad + \text{Tr} \left((\mathbf{E}_i^{(r)})^{-1} \mathbf{V}_i^H \bar{\mathbf{H}}_i^H \mathbf{U}_i^{(r)} \right) \\
 &\quad \left. - \sum_j \text{Tr} \left(\bar{\mathbf{H}}_i^H \mathbf{U}_i^{(r)} (\mathbf{E}_i^{(r)})^{-1} (\mathbf{U}_i^{(r)})^H \bar{\mathbf{H}}_i \mathbf{V}_j \mathbf{V}_j^H \right) \right), \quad (18)
 \end{aligned}$$

where $c_i^{(r)} = -b_i^{(r)} - \sigma^2 \text{Tr}((\mathbf{E}_i^{(r)})^{-1} (\mathbf{U}_i^{(r)})^H \mathbf{U}_i^{(r)})$ is the irrelevant constant term which can be omitted in the following optimization process, and $\mathbf{U}_i^{(r)}$ represents $\mathbf{U}_i^{\text{mmse}}$ with fixed beamformer $\mathbf{V}_i^{(r)}$.

Since the above function is convex with respect to \mathbf{V}_i , the optimal solution of \mathbf{V}_i can be obtained by taking the Lagrange multiplier method. Note that the beamformers from the serving UAVs to the user need to be obtained one by one, so that the Lagrange function is required to be decoupled as the function of \mathbf{V}_{ik} , denoted as (19), shown at the bottom of the next page, where $\mu_{km} \geq 0$ is the introduced Lagrangian multiplier associated with the power constraint of m -th antenna of the k -th UAV and $\left[\sum_{i=1}^I \mathbf{V}_{ik} \mathbf{V}_{ik}^H \right]_{m,m}$ can also be expressed as $\sum_{i=1}^I \mathbf{p}_m^H \mathbf{V}_{ik} \mathbf{V}_{ik}^H \mathbf{p}_m$ where

$$\mathbf{p}_m = \left[0, \dots, \underset{m\text{-th}}{1}, \dots, 0 \right]^T \in \mathbb{C}^{M \times 1}. \quad (20)$$

Note that the constraint C1 in problem (7) takes effect separately for each antenna, so that \mathbf{p}_m is introduced to take out the term associated with the m -th antenna. Recall the assumption that for each user only the channel matrices towards their serving UAVs are known in the serving cluster. Thus, the optimization for beamforming matrices that are not in a particular user's serving cluster is meaningless to that user. By substituting $\mathbf{p}_m^H \mathbf{V}_{ik} \mathbf{V}_{ik}^H \mathbf{p}_m$ into the Lagrange function (19), the optimal \mathbf{V}_{ik} can be further obtained according to the Lagrange's first-order optimization conditions, denoted as

$$\mathbf{V}_{ik}^{(r+1)} = \mathbf{\Gamma}_k^{-1} \mathbf{\Phi}_{ik}, \text{ if } k \in C_i, \quad (21)$$

$$\mathbf{V}_{ik}^{(r+1)} = \mathbf{0}, \text{ if } k \notin C_i, \quad (22)$$

where

$$\begin{aligned}
 \mathbf{\Gamma}_k &= \sum_{i=1}^I \bar{\mathbf{H}}_{ik}^H \mathbf{U}_i^{(r)} (\mathbf{E}_i^{(r)})^{-1} (\mathbf{U}_i^{(r)})^H \bar{\mathbf{H}}_{ik} + \sum_{m=1}^M \mu_{km} \mathbf{p}_m \mathbf{p}_m^H, \\
 \mathbf{\Phi}_{ik} &= \bar{\mathbf{H}}_{ik}^H \mathbf{U}_i^{(r)} (\mathbf{E}_i^{(r)})^{-1} \\
 &\quad - \sum_{l \neq k, l \in C_i} \left(\sum_{i=1}^I \bar{\mathbf{H}}_{il}^H \mathbf{U}_i^{(r)} (\mathbf{E}_i^{(r)})^{-1} (\mathbf{U}_i^{(r)})^H \bar{\mathbf{H}}_{il} \right) \mathbf{V}_{il}^{(r)}.
 \end{aligned}$$

The beamforming matrix \mathbf{V}_{ik} can be expressed as a function of $\boldsymbol{\mu}_k = [\mu_{k1}, \mu_{k2}, \dots, \mu_{kM}]^T$, denoted as $\mathbf{V}_{ik}(\boldsymbol{\mu}_k)$ in the following and the Lagrange multiplier μ_{km} is used to satisfy the complementary slackness condition for the power constraint:

$$\mu_{km} \left(\left[\sum_{i=1}^I \mathbf{V}_{ik}(\boldsymbol{\mu}_k) \mathbf{V}_{ik}(\boldsymbol{\mu}_k)^H \right]_{m,m} - P_{km} \right) = 0. \quad (23)$$

It should be noted that, when

$$\mathbf{Q}_k = \sum_{i=1}^I \bar{\mathbf{H}}_{ik}^H \mathbf{U}_i^{(r)} (\mathbf{E}_i^{(r)})^{-1} (\mathbf{U}_i^{(r)})^H \bar{\mathbf{H}}_{ik} \quad (24)$$

is a positive definite matrix and full rank, it can be decomposed as

$$\mathbf{Q}_k = \mathbf{D}_k \mathbf{\Lambda}_k \mathbf{D}_k^H, \quad (25)$$

based on the singular value decomposition (SVD), where $\mathbf{Q}_k \mathbf{Q}_k^H = \mathbf{Q}_k^H \mathbf{Q}_k = \mathbf{I}_M$ and $\mathbf{\Lambda}_k$ is a diagonal matrix with positive diagonal elements. In this case, if

$$\left[\sum_{i=1}^I \mathbf{V}_{ik}(\mathbf{0}) \mathbf{V}_{ik}(\mathbf{0})^H \right]_{m,m} \leq P_{km}, \quad (26)$$

then the optimal $\mathbf{V}_{ik} = \mathbf{V}_{ik}(\mathbf{0})$. Otherwise, to satisfy the per-antenna power constraint, the beamformer must meet the following condition:

$$\left[\sum_{i=1}^I \mathbf{V}_{ik} \mathbf{V}_{ik}^H \right]_{m,m} = P_{km}, \quad (27)$$

and it is equivalent to

$$\left[\left(\mathbf{\Lambda}_k + \sum_{m=1}^M \mu_{km} \mathbf{p}_m \mathbf{p}_m^H \right)^{-2} \mathbf{\Theta}_k \right]_{m,m} = P_{km}, \quad (28)$$

where

$$\mathbf{\Theta}_k = \mathbf{D}_k^H \left(\sum_{i=1}^I \mathbf{\Phi}_{ik} \mathbf{\Phi}_{ik}^H \right) \mathbf{D}_k. \quad (29)$$

Further, the equation (28) can be reformulated as

$$\frac{[\mathbf{\Theta}_k]_{m,m}}{([\mathbf{\Lambda}_k]_{m,m} + \mu_{km})^2} = P_{km}, \quad (30)$$

and the optimal μ_{km} can be obtained by applying the bisection method. Notice that when $\mu_{km} \rightarrow \infty$, the left side of the

Algorithm 1 The Proposed User-Centric Joint Beamforming Design

- 1 Initialize unblocked UAVG according to i -th user's link condition as cluster $\mathcal{C}_i \subseteq \mathcal{K}, \forall i \in \mathcal{I}$;
- 2 Acquire CSI $\tilde{\mathbf{H}}_{ik}$ in cluster \mathcal{C}_i by (5) for beamforming design;
- 3 Initialize k -th BS's $\{\mathbf{V}_{ik}^{(0)}\}_{\forall k \in \mathcal{C}_i}$ to satisfy constraint C2 in (7), $\forall k \in \mathcal{K}$;
- 4 **repeat**
- 5 Compute $\mathbf{U}_i^{(r)}$ according to (9) with fixed $\mathbf{V}_{ik}^{(r)}$.
- 6 Compute $\mathbf{E}_i^{(r)}$ according to (10) with fixed $\mathbf{U}_i^{(r)}$ and $\mathbf{V}_{ik}^{(r)}$.
- 7 Update $\mathbf{V}_{ik}^{(r+1)}$ by (21) with fixed $\mathbf{U}_i^{(r)}$ and $\mathbf{E}_i^{(r)}$ if $k \in \mathcal{C}_i$, else $\mathbf{V}_{ik}^{(r+1)} = 0$.
- 8 **until** $\|\mathbf{R}_i^{(r+1)} - \mathbf{R}_i^{(r)}\| < \epsilon$ or $r = r_{\max}$;

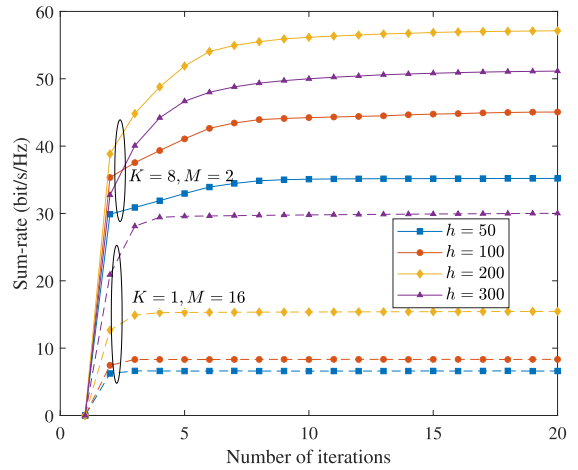


FIGURE 3. The convergence behaviour of the proposed user-centric joint beamforming design with $h \in \{50, 100, 200, 300\}$, $p = 0.4$, $\mathbb{E}[H] = 40$ m.

equation (30) goes to zero and it can be readily verified that it is a monotonically decreasing function [37]. Therefore, the solution of equation (30) is bound to exist, which is denoted as μ_{km}^{opt} . Then, the optimal beamforming matrix can be shown as $\mathbf{V}_{ik}^{\text{opt}} = \mathbf{V}_{ik}(\mu_k^{\text{opt}})$. To be noticed, the upper bound of μ_{km} has to be found first to apply the bisection method, which can be derived as

$$\mu_{km} < \sqrt{\frac{[\Theta_k]_{m,m}}{P_{km}}} \triangleq \mu_{km}^{\text{ub}}. \quad (31)$$

This is supported by

$$\frac{[\Theta_k]_{m,m}}{([\Lambda_k]_{m,m} + \mu_{km}^{\text{ub}})^2} < \frac{[\Theta_k]_{m,m}}{(\mu_{km}^{\text{ub}})^2} = P_{km}. \quad (32)$$

When \mathbf{Q}_k is low-rank, the above method is not applicable since the \mathbf{D}_k derived by SVD is not a unitary matrix, so the steps in (25) no longer pertain. To address this issue, the first step is to check whether $\mu_{km} = 0$ is the optimal solution or not, similar to (26). If not, the optimal μ_{km} should be a positive value, and we will provide the solution in the following. Here, we assume the rank of \mathbf{Q}_k as $r_k = \text{rank}(\mathbf{Q}_k) < M$. After the SVD operation, \mathbf{Q}_k can be decomposed as

$$\mathbf{Q}_k = [\tilde{\mathbf{D}}_k, \tilde{\mathbf{D}}_k] \text{diag}\{\tilde{\Lambda}_k, \tilde{\Lambda}_k\} [\tilde{\mathbf{D}}_k, \tilde{\mathbf{D}}_k]^H, \quad (33)$$

where $\tilde{\mathbf{D}}_k$ includes the first r_k singular vectors corresponding to the r_k positive eigenvalues in diagonal matrix $\tilde{\Lambda}_k$, and $\tilde{\mathbf{D}}_k$ contains the remaining $M - r_k$ singular vectors corresponding

to the $M - r_k$ zero-valued eigenvalues in matrix $\tilde{\Lambda}_k$. By defining $\mathbf{D}_k \triangleq [\tilde{\mathbf{D}}_k, \tilde{\mathbf{D}}_k]$, similar to the steps from (27) to (30), we can obtain that when $0 < m \leq r_k$, the solution of the following equation can be derived with the optimal μ_{km} found by utilizing the bisection method:

$$\left[\sum_{i=1}^I \mathbf{v}_{ik}(\mu_k) \mathbf{v}_{ik}(\mu_k)^H \right]_{m,m} = \frac{[\Theta_k]_{m,m}}{([\Lambda_k]_{m,m} + \mu_{km}^{\text{ub}})^2} = P_{km}. \quad (34)$$

When $r_k < m \leq M$, the optimal μ_{km} should be obtained by searching the solution of the following equation:

$$\left[\sum_{i=1}^I \mathbf{v}_{ik}(\mu_k) \mathbf{v}_{ik}(\mu_k)^H \right]_{m,m} = \frac{[\Theta_k]_{m,m}}{(\mu_{km}^{\text{ub}})^2} = P_{km}. \quad (35)$$

Based on the aforementioned analysis, the sum-rate maximization problem (7) can be solved by alternately optimizing $\mathbf{V}_{ik}^{(r)}$, $\mathbf{E}_i^{(r)}$ and $\mathbf{U}_i^{(r)}$, which is summarized in Algorithm 8. Let us analyze the complexity of the proposed algorithm. The main complexity mainly lies in Step 4, the iteration process, which contains three parts. First, the complexity of computing $\mathbf{U}_i^{(r)}$ according to (9) for all users is $\mathcal{O}(IN^3)$. Second, the complexity of computing the MSE matrix $\mathbf{E}_i^{(r)}$ according to (10) can be ignored because the $\mathbf{U}_i^{(r)}$ calculated in of the previous step can be directly utilized without recomputing the inverse matrix. Third, the complexity of computing beamforming matrices $\mathbf{V}_{ik}^{(r+1)}$ is related to the number of UAVs in each user's serving cluster, which can be assumed as C . The complexity of the third part

$$\begin{aligned} \mathcal{L}(\mathbf{V}_{ik}, \mu_{km}) = & \text{Tr}(-(\mathbf{E}_i^{(r)})^{-1}(\mathbf{U}_i^{(r)})^H \tilde{\mathbf{H}}_i \mathbf{V}_i - (\mathbf{E}_i^{(r)})^{-1} \mathbf{V}_i^H \tilde{\mathbf{H}}_i^H \mathbf{U}_i^{(r)} + \sum_j (\mathbf{E}_j^{(r)})^{-1} (\mathbf{U}_j^{(r)})^H \tilde{\mathbf{H}}_j \mathbf{V}_j \mathbf{V}_j^H \tilde{\mathbf{H}}_j^H \mathbf{U}_j^{(r)}) \\ & + \sum_{m=1}^M \mu_{km} \left(\left[\sum_{i=1}^I \mathbf{v}_{ik} \mathbf{v}_{ik}^H \right]_{m,m} - P_{km} \right), \end{aligned} \quad (19)$$

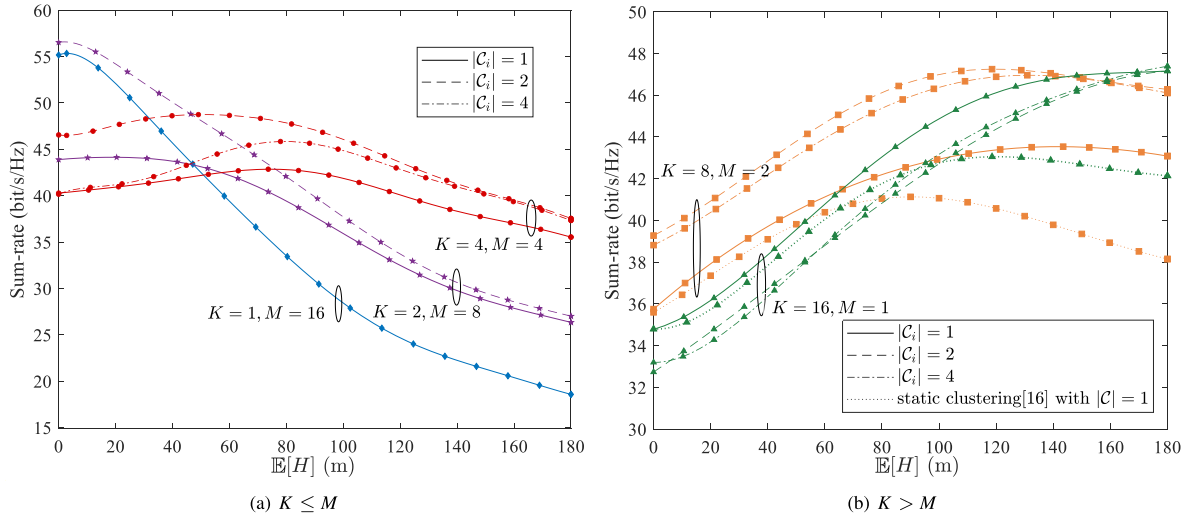


FIGURE 4. Sum-rate versus average height of buildings $\mathbb{E}[H]$ for different UAV parameters with cluster size $|C_i| \in \{1, 2, 4\}$, $h = 250$ m, $\rho = 0.2$: (a) $K \leq M$; (b) $K > M$.

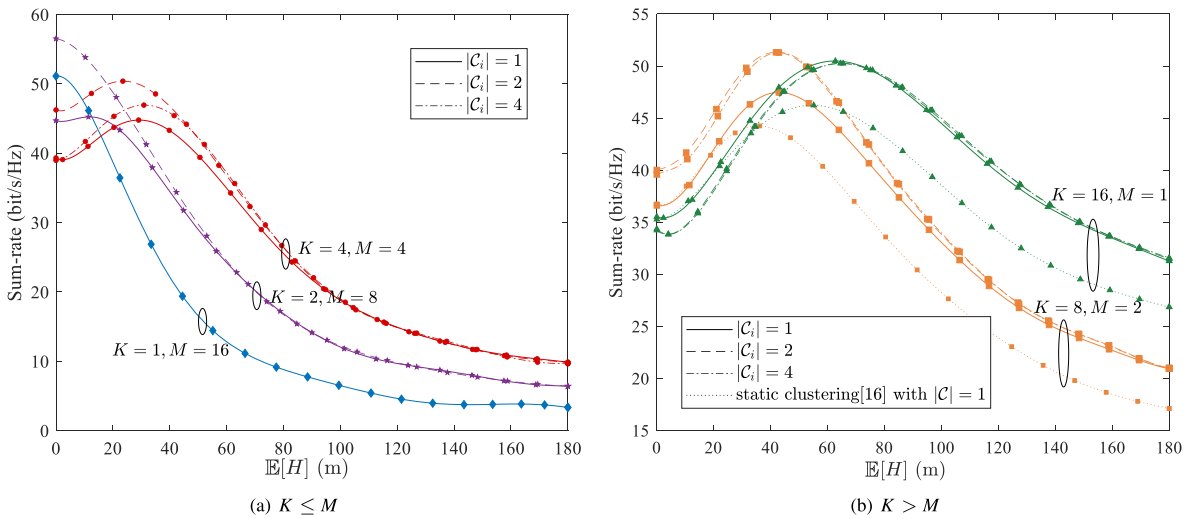


FIGURE 5. Sum-rate versus average height of buildings $\mathbb{E}[H]$ for different UAV parameters with cluster size $|C_i| \in \{1, 2, 4\}$, $h = 250$ m, $\rho = 0.8$: (a) $K \leq M$; (b) $K > M$.

is $\mathcal{O}(CI(r_{max}^3 + M^3))$, where r_{max} is the maximum value of r . The overall complexity is given by $\mathcal{O}(I(C(r_{max}^3 + M^3) + N^3))$.

IV. PERFORMANCE EVALUATION

The simulation is based on the scenario that UAVs and users are randomly placed in a square area with 2×2 kilometers and the orientations of buildings are distributed uniformly in range $(0, 2\pi]$ with their lengths and widths set to 200 meters and 40 meters, respectively. The number of users is $I = 16$ and the number of the receive antennas is $N = 2$. There are $M_0 = 16$ antennas in total and the per-antenna transmitting power P_{km} is limited to 24 dBm. The channel gain of the UAV-user link, denoted by $g_{i,k,l}$ in (3), can be modeled as $g_{i,k,l} = \sqrt{\beta_0 d_{i,k}^{-\alpha}} \left(\sqrt{\frac{\kappa_{i,k,l}}{1+\kappa_{i,k,l}}} \tilde{g}_{i,k,l} + \sqrt{\frac{1}{1+\kappa_{i,k,l}}} \tilde{g}_{i,k,l} \right)$, where $\beta_0 = -30$ dB is the path loss at the reference distance $d_0 = 1$ m, $d_{i,k}$ denotes the distance between UAV k and user i , α is the path loss exponent, $\kappa_{i,k,l}$ is the Rician factor of path l from UAV k to user i , $|\tilde{g}_{i,k,l}| = 1$, and $\tilde{g}_{i,k,l} \sim \mathcal{CN}(0, 1)$.

Here, we assume $\alpha = 4$, $\kappa_{i,k,1} = 10$, $\kappa_{i,k,2} = 5$, $\kappa_{i,k,3} = 3$, $L_{ik} = L = 3$, $\forall i, k$ [38] and for simplicity, we set the number of data streams d_i to 1. For generality, the following results are obtained by averaging over 200 Monte Carlo trials with random locations of UAVs and users. Besides, $d_{max} = 20$ and $\epsilon = 10^{-3}$.

The convergence behaviour of the proposed beamforming design is first studied and shown in Fig. 3. It is observed that the distributed deployment of antennas, i.e., $K = 8$, outperforms the centralized one, i.e., $K = 1$, in this scene when $p = 0.4$ and $\mathbb{E}[H] = 40$ m. In addition, when $K = 1$, the sum-rate increases as h goes higher, but when $K = 8$, it increases at first and then decreases and the convergence speed slows down slightly as h goes higher. This is due to the fact that as the UAV flies higher it can provide service to more users so that more optimization variables are involved. Nevertheless, in all cases, the proposed algorithm converges fast which confirms the practical benefits of the algorithm,

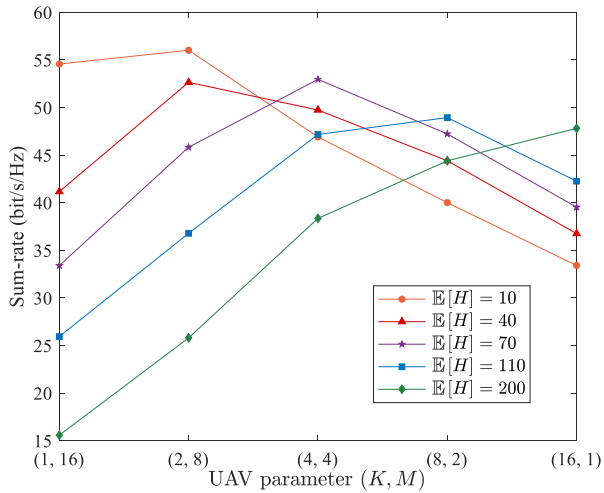


FIGURE 6. Sum-rate versus UAV parameters under different buildings' average height $\mathbb{E}[H]$.

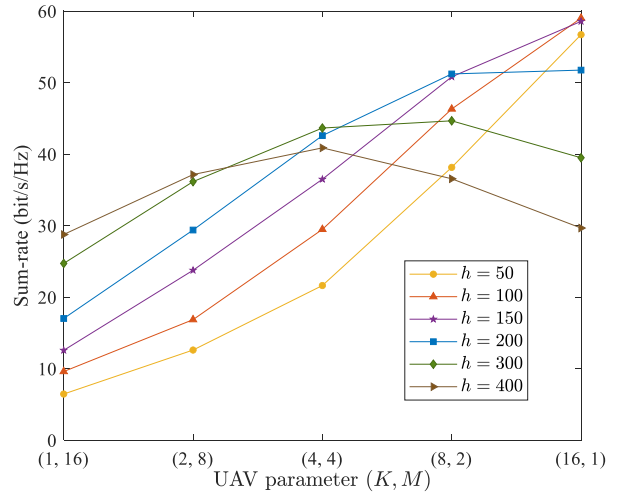


FIGURE 8. Sum-rate versus UAV parameters under different UAV height h .

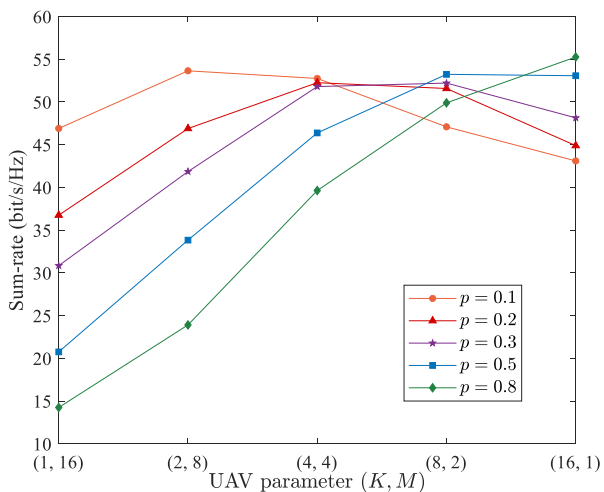


FIGURE 7. Sum-rate versus UAV parameters under different buildings' coverage ratio p .

therefore, as mentioned above, the max number of algorithm iterations d_{\max} is set to 20, which can be validated to be convergent by this figure.

Figs. 4-5 illustrates the sum-rate of different UAV parameters under different building scenes and cluster sizes $|\mathcal{C}_i| \in \{1, 2, 4\}$. Fig. 4(a) and Fig. 5(a) show the cases with fewer UAVs and more antennas per UAV, i.e., $K \leq M$, which are regarded as the centralized deployments. From the aforementioned subfigures, for the deployments with a higher degree of centralization, such as the deployment with $K = 1, M = 16$, their performance decreases more rapidly as average building height increases. For the deployments with a lower degree of centralization, such as the deployment with $K = 4, M = 4$, although the performance is also degraded by building obstructions, it performs better than highly centralized deployments in terms of the scenarios with higher average building heights. This trend is more obviously shown in Fig. 4(a), where the building density p is higher. Fig. 4(b) and Fig. 5(b) show the scenarios with more UAVs and less antenna per UAV, i.e., $K > M$, which are regarded

as distributed deployments. In Fig. 4(b), where the building density p is lower, the performance rises with the average building height within a certain range. In scenarios with more severe blocking effects, which are shown in Fig. 5(b), the balancing capabilities of user-centric deployments will meet their limits sooner, as shown at the top of the performance curves. From another perspective to Figs. 4-5, it can be seen that with the user-centric joint beamforming, the distributed antenna deployments ($K \geq 2$) reached a higher sum-rate than the centralized deployment ($K = 1$) in dense urban areas. The proposed user-centric design performs better than the traditional static clustering [20] where users can only be served by the UAVs within some certain fixed range with serving cluster size $|\mathcal{C}_i| = 1$ and the gain becomes more pronounced as the blockage effect becomes severer. Besides, comparing the two figures, as p grows, the user-centric deployment outperforms the centralized one under lower $\mathbb{E}[H]$ with the trend that it increases at first then decreases as $\mathbb{E}[H]$ increases, since the blockage can reduce interference brought by other UAVs, thus resulting in better performance. In addition, the sum-rate benefits from the increase of $|\mathcal{C}_i|$ thanks to joint transmission. In spite of the great benefit brought by the distributed strategy, under some circumstances, increasing the cluster can bring higher gain than increasing the number of UAVs, which can avoid higher cost and energy consumption problems brought by multiple UAVs.

Fig. 6 shows that the optimal antenna deployment is related to the average height of buildings. As $\mathbb{E}[H]$ increases, the advantage of distributed deployment becomes more obvious since the more distributed the antennas are, the more likely the user is to get service under high-rise environments, but the overall performance is still affected by the severer blockages.

Fig. 7 depicts the impact of p on sum-rate under different antenna deployments. Similar to Fig. 5, there is a relationship between the UAV optimal deployment and p , that is, the user-centric joint beamforming with distributed antennas achieves higher performance than centralized systems due to

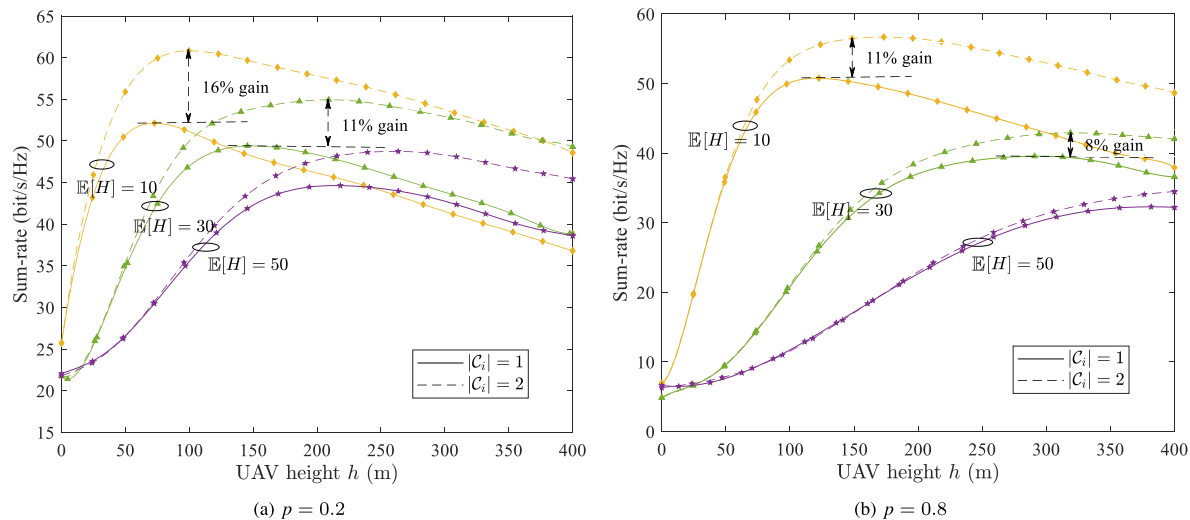


FIGURE 9. Sum-rate versus UAV height h with different cluster sizes under different kinds of blockage parameters $p \in \{0.2, 0.8\}$, $\mathbb{E}[H] \in \{10, 30, 50\}$.

the higher blockage probability, but since a more distributed antenna deployment lower the transmit power for user serving under a fixed cluster, it will not have better performance unless in extremely dense scenes. It is observed that the increase of p barely influences the optimal performance thanks to the distributed gain.

From Fig. 8, we can find the systems of different deployments perform diversely as the height of UAV h grows. The centralized one gets better performance when UAV flies higher since more users could get service and the factor is predominant despite the path loss caused by greater distance. However, for the distributed one, flying higher could not increase so many connections for system gain and the path loss becomes the predominant factor, so there exists an optimal UAV height related to different deployments and the sum-rate decreases when h gets bigger.

In Fig. 9, the performance curves under different $\mathbb{E}[H]$ and p with the variation of UAV height h are plotted, where $K = 2$, $M = 8$. Fig. 9(a) shows the scenes with low building density p while Fig. 9(b) shows the scenes with high p . As expected, there exists an optimal value for the UAV height, and the optimal height grows with the increase of $\mathbb{E}[H]$ or p . This is because facing with taller and denser buildings, UAVs need to fly higher to decrease the blocking effect. However, when they are over a certain height, the reduction of blocking has reached its limit, and continuing to increase the flight altitude will only significantly increase the path loss. At the same time, when $|C_i|$ increases from 1 to 2, the optimal height grows as well, and the increase of cluster size achieves obvious gain which varies with different $\mathbb{E}[H]$ and p , and the gain increases with the decrease of blockage effect.

V. CONCLUSION

In this article, we propose a user-centric UAV joint beamforming to guarantee user services under dense urban areas where the blockage effect is modeled by exploiting the 3D relationship among the user, buildings, and object UAV-BS.

A user-centric joint beamforming design for multi-UAV networks is proposed under the 3D blockage effect, aiming at maximizing the sum-rate performance of the system, where the distributed scheme of the antenna configuration is employed within user-centric UAV clusters. To investigate the cost-effective UAV configuration parameters, the per-antenna power constraint is adopted to satisfy many transmission operations of practical interest. Simulation results have provided guidance in optimal UAV configurations and beamformer design under the impact of blockages.

REFERENCES

- [1] M. Mozaffari, W. Saad, M. Bennis, Y.-H. Nam, and M. Debbah, "A tutorial on UAVs for wireless networks: Applications, challenges, and open problems," *IEEE Commun. Surveys Tuts.*, vol. 21, no. 3, pp. 2334–2360, 3rd Quart., 2019.
- [2] Y. Zeng, R. Zhang, and T. J. Lim, "Wireless communications with unmanned aerial vehicles: Opportunities and challenges," *IEEE Commun. Mag.*, vol. 54, no. 5, pp. 36–42, May 2016.
- [3] H. Shakhathreh, A. H. Sawalmeh, A. Al-Fuqaha, Z. Dou, E. Almaita, I. Khalil, N. S. Othman, A. Khreishah, and M. Guizani, "Unmanned aerial vehicles (UAVs): A survey on civil applications and key research challenges," *IEEE Access*, vol. 7, pp. 48572–48634, 2019.
- [4] J. Liu and H. Zhang, "Height-fixed UAV enabled energy-efficient data collection in RIS-aided wireless sensor networks," *IEEE Trans. Wireless Commun.*, vol. 22, no. 11, pp. 7452–7463, Nov. 2023.
- [5] H. Wei and H. Zhang, "Equivalent modeling and analysis of handover process in K-tier UAV networks," *IEEE Trans. Wireless Commun.*, vol. 22, no. 12, pp. 9658–9671, Dec. 2023.
- [6] Y. Zeng, J. Lyu, and R. Zhang, "Cellular-connected UAV: Potential, challenges, and promising technologies," *IEEE Wireless Commun.*, vol. 26, no. 1, pp. 120–127, Feb. 2019.
- [7] L. Zhu, J. Zhang, Z. Xiao, X. Cao, D. O. Wu, and X.-G. Xia, "3-D beamforming for flexible coverage in millimeter-wave UAV communications," *IEEE Wireless Commun. Lett.*, vol. 8, no. 3, pp. 837–840, Jun. 2019.
- [8] Y. Huang, Q. Wu, R. Lu, X. Peng, and R. Zhang, "Massive MIMO for cellular-connected UAV: Challenges and promising solutions," *IEEE Commun. Mag.*, vol. 59, no. 2, pp. 84–90, Feb. 2021.
- [9] M. Nafees, J. Thompson, and M. Safari, "Multi-tier variable height UAV networks: User coverage and throughput optimization," *IEEE Access*, vol. 9, pp. 119684–119699, 2021.
- [10] H. He, S. Zhang, Y. Zeng, and R. Zhang, "Joint altitude and beamwidth optimization for UAV-enabled multiuser communications," *IEEE Commun. Lett.*, vol. 22, no. 2, pp. 344–347, Feb. 2018.

- [11] H. Niu, X. Zhao, and J. Li, "3D location and resource allocation optimization for UAV-enabled emergency networks under statistical QoS constraint," *IEEE Access*, vol. 9, pp. 41566–41576, 2021.
- [12] L. Yang, H. Zhang, and Y. He, "Temporal correlation and long-term average performance analysis of multiple UAV-aided networks," *IEEE Internet Things J.*, vol. 8, no. 11, pp. 8854–8864, Jun. 2021.
- [13] C. Zhang, L. Zhang, L. Zhu, T. Zhang, Z. Xiao, and X.-G. Xia, "3D deployment of multiple UAV-mounted base stations for UAV communications," *IEEE Trans. Commun.*, vol. 69, no. 4, pp. 2473–2488, Apr. 2021.
- [14] J. Ji, L. Cai, K. Zhu, and D. Niyato, "Decoupled association with rate splitting multiple access in UAV-assisted cellular networks using multi-agent deep reinforcement learning," *IEEE Trans. Mobile Comput.*, vol. 23, no. 3, pp. 2186–2201, Mar. 2024.
- [15] Y.-H. Hsu and R.-H. Gau, "Reinforcement learning-based collision avoidance and optimal trajectory planning in UAV communication networks," *IEEE Trans. Mobile Comput.*, vol. 21, no. 1, pp. 306–320, Jan. 2022.
- [16] V. Saxena, J. Jaldén, and H. Klessig, "Optimal UAV base station trajectories using flow-level models for reinforcement learning," *IEEE Trans. Cognit. Commun. Netw.*, vol. 5, no. 4, pp. 1101–1112, Dec. 2019.
- [17] D. Wu and H. Zhang, "Tractable modelling and robust coordinated beamforming design with partially accurate CSI," *IEEE Wireless Commun. Lett.*, vol. 10, no. 11, pp. 2384–2387, Nov. 2021.
- [18] Y. Zhu, D. Wu, and H. Zhang, "Tunable SRS-aware robust coordinated beamforming design with channel aging," *IEEE Trans. Veh. Technol.*, vol. 72, no. 12, pp. 16754–16759, Dec. 2023.
- [19] R. W. Heath Jr. and A. Lozano, *Foundations of MIMO Communication*. Cambridge, U.K.: Cambridge Univ. Press, 2018.
- [20] L. Liu, S. Zhang, and R. Zhang, "CoMP in the sky: UAV placement and movement optimization for multi-user communications," *IEEE Trans. Commun.*, vol. 67, no. 8, pp. 5645–5658, Aug. 2019.
- [21] H. Park, T.-H. Nguyen, and L. Park, "Federated deep learning for RIS-assisted UAV-enabled wireless communications," in *Proc. 13th Int. Conf. Inf. Commun. Technol. Converg. (ICTC)*, Oct. 2022, pp. 831–833.
- [22] M.-L. Tham, Y. J. Wong, A. Iqbal, N. B. Ramli, Y. Zhu, and T. Dagiuklas, "Deep reinforcement learning for secrecy energy-efficient UAV communication with reconfigurable intelligent surface," in *Proc. IEEE Wireless Commun. Netw. Conf. (WCNC)*, Mar. 2023, pp. 1–6.
- [23] C. Pan, H. Ren, K. Wang, J. F. Kolb, M. ElKashlan, M. Chen, M. Di Renzo, Y. Hao, and J. Wang, "Reconfigurable intelligent surfaces for 6G systems: Principles, applications, and research directions," *IEEE Commun. Mag.*, vol. 59, no. 6, pp. 14–20, Jun. 2021.
- [24] Y. Lin, R. Zhang, C. Li, L. Yang, and L. Hanzo, "Graph-based joint user-centric overlapped clustering and resource allocation in ultradense networks," *IEEE Trans. Veh. Technol.*, vol. 67, no. 5, pp. 4440–4453, May 2018.
- [25] J. Kim, H.-W. Lee, and S. Chong, "Virtual cell beamforming in cooperative networks," *IEEE J. Sel. Areas Commun.*, vol. 32, no. 6, pp. 1126–1138, Jun. 2014.
- [26] H. Zhang, Y. Chen, and Z. Han, "Explicit modelling and performance analysis of cell group selection with backhaul-aware biasing," *IEEE Wireless Commun. Lett.*, vol. 8, no. 1, pp. 273–276, Feb. 2019.
- [27] W. Huang, J. Peng, and H. Zhang, "User-centric intelligent UAV swarm networks: Performance analysis and design insight," *IEEE Access*, vol. 7, pp. 181469–181478, 2019.
- [28] P. Dinh, T. M. Nguyen, S. Sharafeddine, and C. Assi, "Joint location and beamforming design for cooperative UAVs with limited storage capacity," *IEEE Trans. Commun.*, vol. 67, no. 11, pp. 8112–8123, Nov. 2019.
- [29] W. Tang, H. Zhang, Y. He, and M. Zhou, "Performance analysis of multi-antenna UAV networks with 3D interference coordination," *IEEE Trans. Wireless Commun.*, vol. 21, no. 7, pp. 5145–5161, Jul. 2022.
- [30] W. Tang, H. Zhang, and Y. He, "Tractable modelling and performance analysis of UAV networks with 3D blockage effects," *IEEE Wireless Commun. Lett.*, vol. 9, no. 12, pp. 2064–2067, Dec. 2020.
- [31] W. Tang, H. Zhang, and Y. He, "Performance analysis of power control in urban UAV networks with 3D blockage effects," *IEEE Trans. Veh. Technol.*, vol. 71, no. 1, pp. 626–638, Jan. 2022.
- [32] D. Alkama, M. Azni, M. A. Ouamri, and X. Li, "Modeling and performance analysis of vertical heterogeneous networks under 3D blockage effects and multiuser MIMO systems," *IEEE Trans. Veh. Technol.*, early access, Feb. 16, 2024, doi: [10.1109/TVT.2024.3366655](https://doi.org/10.1109/TVT.2024.3366655).
- [33] H. Iimori, G. T. F. de Abreu, O. Taghizadeh, R.-A. Stoica, T. Hara, and K. Ishibashi, "Stochastic learning robust beamforming for millimeter-wave systems with path blockage," *IEEE Wireless Commun. Lett.*, vol. 9, no. 9, pp. 1557–1561, Sep. 2020.
- [34] Y.-F. Liu, Y.-H. Dai, and Z.-Q. Luo, "Coordinated beamforming for MISO interference channel: Complexity analysis and efficient algorithms," *IEEE Trans. Signal Process.*, vol. 59, no. 3, pp. 1142–1157, Mar. 2011.
- [35] Q. Shi, M. Razaviyayn, Z.-Q. Luo, and C. He, "An iteratively weighted MMSE approach to distributed sum-utility maximization for a MIMO interfering broadcast channel," *IEEE Trans. Signal Process.*, vol. 59, no. 9, pp. 4331–4340, Sep. 2011.
- [36] Y. Sun, P. Babu, and D. P. Palomar, "Majorization-minimization algorithms in signal processing, communications, and machine learning," *IEEE Trans. Signal Process.*, vol. 65, no. 3, pp. 794–816, Feb. 2017.
- [37] C. Pan, H. Ren, K. Wang, W. Xu, M. ElKashlan, A. Nallanathan, and L. Hanzo, "Multicell MIMO communications relying on intelligent reflecting surfaces," *IEEE Trans. Wireless Commun.*, vol. 19, no. 8, pp. 5218–5233, Aug. 2020.
- [38] J. Liu and H. Zhang, "Multi-branch unsupervised learning-based beamforming in mm-wave massive MIMO systems with inaccurate information," *IEEE Trans. Green Commun. Netw.*, early access, May 15, 2024, doi: [10.1109/TGCN.2024.3401575](https://doi.org/10.1109/TGCN.2024.3401575).



XIANMING ZHAO received the B.S., M.S., and Ph.D. degrees in communication and electronic systems from Harbin Institute of Technology. He was the Deputy Director and an Associate Professor with the Teaching and Research Office of Communication Engineering, Harbin Institute of Technology. In 1998, he joined ZTE, dedicating himself to the long-term research and industrial application of wireless access network technology.

As a technological leader, he played a pivotal role in the entire process of research and development and industrialization of 2G/3G/4G/5G technologies. Since 2018, he has been with Harbin Institute of Technology, establishing the Future Information Technology Research Institute. He is leading the development of the world's first 5G (sub 6G + millimeter-wave) and Wi-Fi six integrated high-bandwidth base station system, along with ongoing research in ultra-wideband terahertz communication technology. He has been honored with eight national-level awards, 12 provincial-level awards, including three National Science and Technology Progress Awards.



YUTING ZHU (Student Member, IEEE) received the B.S. degree in communication engineering from Beijing University of Posts and Telecommunications (BUPT), Beijing, China, in 2022, where she is currently pursuing the M.S. degree in communication and information engineering with the School of Artificial Intelligence. Her research interests include the emerging technologies of B5G&6G wireless communication networks and algorithm design.



HONGTAO ZHANG (Senior Member, IEEE) received the Ph.D. degree in communication and information systems from Beijing University of Posts and Telecommunications (BUPT), Beijing, China, in 2008. He is currently a Full Professor with BUPT. He has published more than 100 papers on international journals and conferences, and has filed more than 50 patents. He is the author of ten technical books. His research interests include B5G&6G wireless communication and signal processing.

• • •